NANO LETTERS

Letter

pubs.acs.org/NanoLett

Hierarchical or Not? Effect of the Length Scale and Hierarchy of the Surface Roughness on Omniphobicity of Lubricant-Infused Substrates

Philseok Kim,*[,†,‡] Michael J. Kreder,[†] Jack Alvarenga,[†] and Joanna Aizenberg*[,†,‡,§]

[†]Wyss Institute for Biologically Inspired Engineering, [‡]School of Engineering and Applied Sciences, and [§]Department of Chemistry and Chemical Biology, Harvard University, Cambridge, Massachusetts, United States

Supporting Information

ABSTRACT: Lubricant-infused textured solid substrates are gaining remarkable interest as a new class of omni-repellent nonfouling materials and surface coatings. We investigated the effect of the length scale and hierarchy of the surface topography of the underlying substrates on their ability to retain the lubricant under high shear conditions, which is important for maintaining nonwetting properties under application-relevant conditions. By comparing the lubricant loss, contact angle hysteresis, and sliding angles for water and ethanol droplets on flat, microscale, nanoscale, and hierarchically textured surfaces subjected to various spinning rates (from 100 to 10 000 rpm), we show that lubricant-infused textured surfaces with uniform nanofeatures provide the most shear-tolerant liquid-repellent behavior, unlike lotus leaf-inspired superhydrophobic surfaces, which generally favor hierarchical structures for improved pressure stability and low contact angle hysteresis. On the basis of these findings, we present generalized, low-cost, and scalable methods to manufacture uniform or regionally patterned nanotextured coatings on arbitrary materials and complex shapes. After functionalization and lubrication, these coatings show robust, shear-tolerant omniphobic behavior, transparency, and nonfouling properties against highly contaminating media.

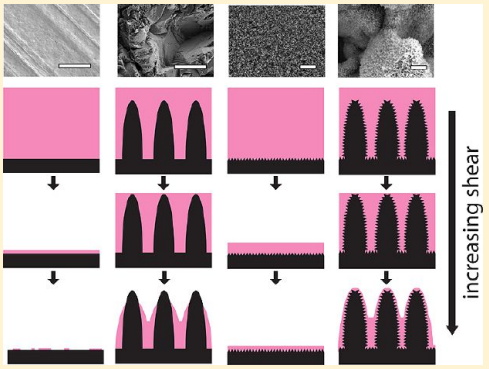

KEYWORDS: *Nanostructure, omniphobic surface, slippery liquid-infused porous surfaces, hierarchical nanostructure, boehmite*

Nonfouling, anti-icing, antibacterial, easy-to-clean, and self-cleaning surfaces are important for maximizing the energy efficiency of building and construction materials, marine vessels, automobiles, aircraft, refrigeration units, wind turbines, air and water filtration/purification processes, medical devices, and household care that collectively are responsible for global revenue expected to reach $3.8 billion USD by 2017.[1] During the past two decades, superhydrophobic nanocoatings that are inspired by the lotus-leaf effect have been extensively studied for these purposes.[2−14] However, these surfaces rely on trapped air to repel liquids, which is prone to escape under conditions involving high temperature, pressure, humidity, and when exposed to low-surface-tension liquids.[15,16] This results in an unavoidable failure of their liquid-repelling function. While both microstructure and nanostructure alone can still provide superhydrophobicity, it has been shown that superhydrophobic surfaces with hierarchical, multitiered structures combining the distinct and complementary role of microstructure (pressure dissipation) and nanostructure (high capillary pressure) can further decrease contact angle hysteresis (CAH, the difference of advancing and receding contact angle) and increase pressure tolerance critical for self-cleaning property and robustness of such surfaces.[17−25] In addition to robust superhydrophobicity, they begin to offer oleophobic properties and typically have higher contact angles, lower sliding angles, and lower contact angle hysteresis[26,27] than single-tiered structured surfaces.[4−6] However, they still fail under pressure, at high or low temperatures, or in a humid environment.[28,29]

To overcome the shortcomings of the lotus-leaf-inspired materials, a new type of *Nepenthes* pitcher plant-inspired materials called slippery liquid infused porous surfaces (SLIPS) has been introduced recently that exhibit antiwetting behavior to almost all fluids and show extreme temperature and pressure stability.[30−35] Unlike superhydrophobic surfaces, SLIPS do not rely on air trapped inside highly porous structures to repel foreign fluids. Instead, a thin layer of a liquid lubricant is trapped inside the porous structures that presents an ultrasmooth, continuous, and chemically homogeneous overlying liquid interface, which provides an extremely slippery, low-hysteresis, nonwetting surface to a broad range of fluids and solids. Moreover, these surfaces display inherent self-healing and repairable properties by restoring the damaged area through the redistribution of the liquid lubricant.[30] To form stable SLIPS, the underlying solid was shown to require a structured top layer whose functionalized surfaces match the

Received: January 30, 2013
Revised: March 1, 2013

   dx.doi.org/10.1021/nl4003969 | *Nano Lett.* XXXX, XXX, XXX−XXX

chemical nature of the lubricant and its porous network holds the lubricant in place through capillarity. However, most practical applications of nonwetting and antifouling surfaces face environmental shear stresses from continuous exposure to flow of air or other foreign fluids that can act against capillarity, which is holding the lubricant, and compromise the robustness of SLIPS. Therefore, it is critical to understand how the length scale of the underlying porous solids influences the performance of SLIPS and whether it can be further improved by using hierarchically structured surfaces, similar to those showing enhanced superhydrophobic properties. Herein, we address these questions by introducing simple and scalable nano- and microscale roughening methods, carry out careful analysis of the SLIPS performance under various shear conditions, and show that, unlike superhydrophobic surfaces, nanostructured solids with a single-scale feature size offer better stability of liquid repellency than two-tiered, hierarchical surfaces. We then present generalized methods of manufacturing robust, shear-tolerant SLIPS on a wide range of materials and shapes and demonstrate their emerging, unmatched multifunctional properties, such as antifouling, anti-icing, anticorrosion, transparency, and easy cleaning.

In order to investigate the effect of the length scale of surface roughness on the performance of SLIPS, we chose aluminum as a model substrate and used sandblasting and boehmite (aluminum oxy hydroxide, AlO(OH)) nanostructure formation as methods to directly create microscale and nanoscale textures, respectively, on an underlying Al substrate. Figure 1 shows

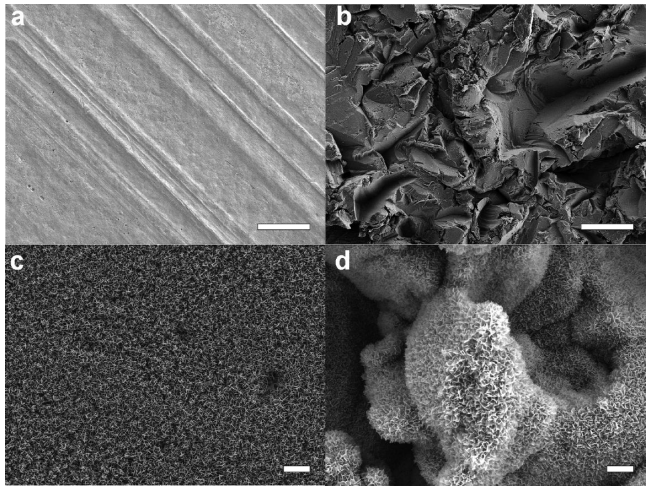

Figure 1. SEM (Scanning Electron Microscope) images of the surface topography of: (a) untreated aluminum, (b) sandblasted microstructured aluminum, (c) nanoscale boehmite on flat aluminum, (d) hierarchical texture of sandblasted and boehmitized aluminum. Scale bars are 50 μm for (a,b) and 1 μm for (c,d).

typical morphologies of the surface features of the native (Figure 1a) and treated (Figure 1b–d) aluminum surfaces. Sandblasting with 120 grit size alumina (avg. particle diameter =125 μm) forms exclusively microscale roughness on the aluminum surface (hereafter labeled "S") with average roughness of 3.2 μm (Figure 1b). Boehmite (hereafter labeled "B"), a reaction product of aluminum and water that has rhombohedral bipyramid crystal structure, was formed by simply boiling the substrate in water.[36,37] The boehmitized surfaces exhibit uniform nanoscale morphology of 10–30 nm-thick crossed leaflets of 50–100 nm in length (Figure 1c). Sandblasted aluminum can also be reacted with water to form boehmite and produce hierarchically structured surface with the combination of nanometer and micrometer features (hereafter labeled "SB") (Figure 1d). All of these surfaces can be readily fluorofunctionalized (hereafter labeled "F" as a suffix) to provide affinity to a fluorinated liquid lubricant that will be infiltrated to form SLIPS. Functionalization was performed by immersing the aluminum substrate in an ethanol or aqueous bath of a surfactant (FS100, phosphate ester with mixed length of fluorinated alkyl chains) or 1H,1H,2H,2H-perfluorooctyl phosphonic acid (F13PA) that showed strong and stable covalent attachment to the native aluminum oxide and boehmite surface (Supporting Information Figure S1).

The performance of these surfaces was characterized by measuring the CAH or the sliding angle of liquid droplets with different surface tensions, which are the properties that characterize the ability to repel various fluids.[38] The CAH values for water and sliding angle for ethanol before and after application of a perfluoropolyether (PFPE) lubricant ("K100"), DuPont Krytox GPL 100 (density = 1.835 g/mL, kinematic viscosity = 12.4 cSt, surface tension = 19 mN/m), are shown in Table 1. A hierarchically structured and fluorinated aluminum

Table 1. Contact Angle Hysteresis of Water and the Sliding Angle of 20 μL Ethanol Droplet Measured at Ambient Conditions on Each Type of Aluminum Substrates before ("Dry") and after the Application of a Perfluoropolyether Lubricant then Draining the Excess Lubricant by Vertically Holding the Substrate for 10 min ("Lubricated").[a]

	contact angle hysteresis (degrees)		ethanol sliding angle (degrees)	
sample name/ surface type	dry	lubricated	dry	lubricated
F/flat	60.6 ± 7.1	9.5 ± 0.9	22.0 ± 0.9	14.2 ± 2.5
SF/microtextured	50.1 ± 4.0	2.3 ± 1.0	52.2 ± 6.9	4.7 ± 0.4
BF/nanotextured	7.9 ± 1.4	2.9 ± 1.6	38.2 ± 3.6	1.6 ± 0.4
SBF/hierarchical	7.5 ± 3.1	3.6 ± 1.0	49.7 ± 3.9	2.5 ± 0.5

[a]F, fluorinated; SF, sandblasted and fluorinated; BF, boehmitized and fluorinated; SBF, sandblasted, boehmitized, and fluorinated. All values reported are a statistical average of five independent measurements.

surface (SBF) and a surface with fluorinated nanoscale roughness (BF) demonstrated better superhydrophobicity than a surface with fluorinated microscale roughness (SF), which is in agreement with previous studies. When these surfaces are infiltrated with a fluorinated lubricant, K100, to form SLIPS (by spreading several drops of lubricant followed by gravity-induced removal of excess lubricant), only the textured surfaces exhibited low CAH (<4°) against both water and ethanol. As indicated by the increase in CAH, a lubricated flat surface loses its liquid-repellent performance, suggesting that in addition to the chemical affinity, at least some level of roughness, especially below the capillary length of the lubricant, is a necessary feature to achieve a stable slippery behavior even under mild forces associated with gravity.

In real applications, even greater shear conditions can be expected which not only oppose the capillarity but also change the effective capillary length of the lubricant. Therefore, we further characterized how the robustness of SLIPS prepared on surfaces with different feature sizes and hierarchy is affected, by subjecting the substrates to high shear and comparing the resultant CAH of liquid droplets. We employed centrifugal

dx.doi.org/10.1021/nl4003969 | Nano Lett. XXXX, XXX, XXX–XXX

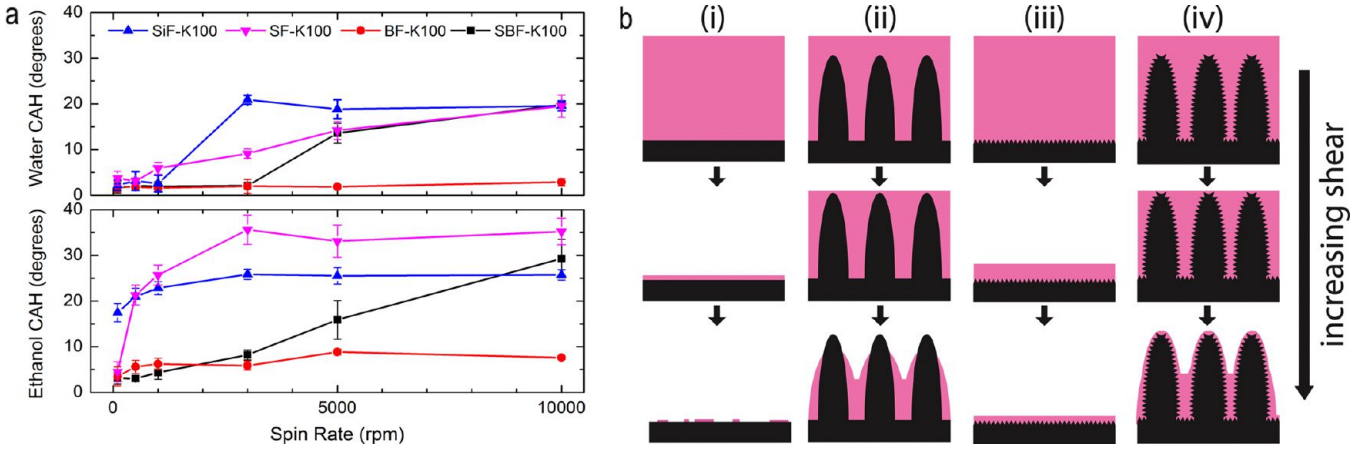

Figure 2. (a) Contact angle hystereses of water (top) and ethanol (bottom) measured on four types of lubricated substrates after spinning for 1 min at each spin rate starting from 100 rpm to 10 000 rpm. SiF (silicon wafer, fluorinated, an ideally flat surface), SF (sandblasted Al, fluorinated, a microscale textured surface), SBF (sandblasted then boehmitized Al, fluorinated, a hierarchically textured surface), and BF (boehmitized Al, fluorinated, a uniformly nanotextured surface). All samples were initially lubricated with excess amount of perfluoropolyether lubricant, K100, to cover the surface. (b) Schematic representations of the evolution of the lubricant thickness and profile with increasing shear on four types of lubricated substrates. (i) flat substrate, (ii) microtextured substrate, (iii) nanostructured substrate, and (iv) hierarchically structured substrate.

force to simulate high shear conditions for four types of lubricated surfaces (flat, microtextured, nanotextured, hierarchical) and compared CAH of water (surface tension = 72.7 mN/m at 298.15 K) and ethanol (surface tension = 22.1 mN/m at 298.15 K) after subjecting the surfaces to different spinning speeds for 60 s in air using a spin coater (Figure 2a). At low spinning rates (up to ∼1000 rpm), all samples showed CAH of <6° for water droplets. As the spinning speed increased, unstructured lubricated surfaces exhibited a sudden increase in CAH reaching >20° at 3000 rpm indicating a rapid deterioration of slipperiness. CAH for SLIPS on microtextured surface showed slow, nearly linear increase reaching ∼20° at 10 000 rpm. In contrast, the surface with only uniform nanoscale roughness preserved excellent water-repellent behavior (i.e., CAH < 3°) up to 10 000 rpm. Surprisingly, the hierarchically structured surface did not provide any advantage over the nanostructured surface and in fact began to show significant deterioration of performance after 3000 rpm. The same, but much more pronounced, trend was observed for the mobility of low-surface-tension ethanol droplets (note that the flat lubricated surface shows high CAH even at 100 rpm). This trend was also confirmed by comparing the average speed of a liquid droplet moving on each type of surfaces (Supporting Information Figure S2). We also measured the weight changes before and after each spinning experiment to calculate the mass of retained lubricant and observed gradual loss of lubricant on all types of surfaces (Supporting Information Table S1). Although microtextured substrates retained more lubricant than nanotextured substrates after subjecting them to a high spinning rate, their performance as SLIPS was worse than that on nanotextured surface indicating that the robustness of SLIPS is not directly correlated to the retention of the lubricant alone.

On the basis of our results, we propose the following mechanisms of the surface evolution under high shear for flat, microstructured, nanostructured, and hierarchical surfaces (Figure 2b). On flat surfaces, thinning of the lubricant layer will lead to exposure of the underlying solid, as there is no capillary force to hold the lubricant (Figure 2b(i)). The length scales of both microtextures and nanotextures we created are much smaller than the capillary length of the PFPE lubricant (∼1 mm under Earth's gravity, g). These surfaces will therefore support a stable overcoating of the lubricant (Figure 2b(ii–iv), top). Under high spinning rates, the acceleration at 2.54 cm from the center of spinning, the point where CAH was measured for each sample, becomes 710 g and 2840 g at 5000 and 10 000 rpm, respectively, and the capillary length of the PFPE lubricant becomes 38.2 and 19.1 μm, respectively. Since some microscale features created by the sandblasting method are larger than these lengths, the PFPE lubricant can be easily lost from the valleys between the larger microscale features under these high acceleration conditions and the underlying solids can be exposed (Figure 2b(ii), bottom). For the case of SLIPS with only relatively uniform nanoscale texture, the lubricant will create a stable smooth overcoating until the thickness of the lubricant layer becomes comparable to the height of the nanoscale features themselves (Figure 2b(iii)). In our experiment, we observed no sign of deterioration of performance up to the spin speed of 10 000 rpm, which corresponds to a ∼400 nm thick lubricant layer on a surface with only nanoscale features that are about 170 nm tall.

Hierarchically textured substrates will therefore show properties between those presented by the micro- and nanostructured surfaces. On one hand, the nanoscale features on top of the microscale features can still provide a large capillary force to hold lubricant and provide a low-surface-energy liquid interface along the microscale topography to prevent contact line pinning (Figure 2b(iv)). On the other hand, the shape of the liquid interface after exposure to a strong shear condition conforms to the microscale topography[39] and is no longer an ideally flat interface required for best performing SLIPS (Figure 2b(iv), bottom). While the droplets did not exhibit irreversible pinning up to the spin rate of 5000 rpm, we observed that the movement of the droplets was slowed down, often resulting in a "stick–slip" behavior with temporary pinning on the substrate during droplet sliding experiments. We attribute this behavior to the kinetic depinning of the droplets owing to the dynamic nature of the liquid interface preserved within the nanotextures, where the triple line tends to find thermodynamically favorable conditions by redistribution of the lubricant and rewetting of

dx.doi.org/10.1021/nl4003969 | Nano Lett. XXXX, XXX, XXX–XXX

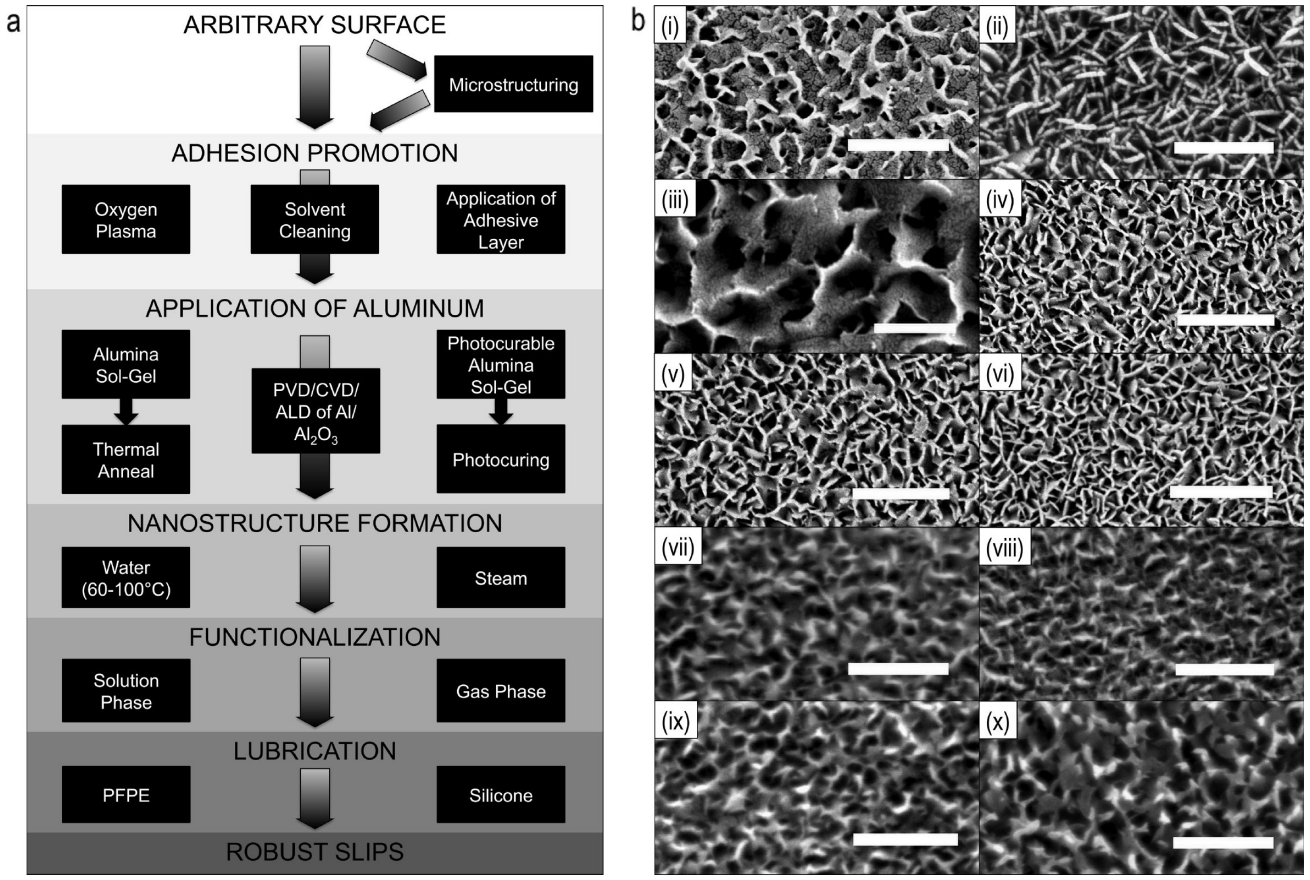

Figure 3. Generalized process for creating boehmite-based SLIPS on arbitrary surfaces. (a) Schematic flowchart; (b) SEM images of boehmite nanostructures on various substrates: (i) glass, (ii) Al 5052, (iii) polystyrene, (iv) polycarbonate, (v) polysulfone, (vi) stainless steel, (vii) acrylic, (viii) nylon, (ix) PVC, (x) PDMS. Scale bars are 500 nm.

the solid substrate. This behavior is typically not observed on traditional superhydrophobic surfaces as the pinning of the liquid droplet on dry, solid surface tends to be permanent and can only overcome the energy barrier when the tilt exceeds the Gibbs inequality.[40] With further increasing spin rate above 5000 rpm, irreversible pinning of droplets was readily observed on SLIPS made on hierarchically textured substrates. We attribute this to the insufficient amount of lubricant remaining on the surface and the lack of associated rearrangement of the lubricant to overcome droplet pinning over a larger microscale feature. Therefore, we can conclude that, unlike superhydrophobic surfaces, robust, stable SLIPS aimed for practical applications, often involving high shear conditions, should be designed to preferentially utilize textured surfaces with only uniform, nanoscale roughness rather than hierarchical features.

Our results show that functionalization and lubrication of boehmitized Al surfaces, which result in consistent, regular nanoscale texture, provide a simple, low-cost, scalable, and environmentally friendly method to convert aluminum, the most abundant metal used for outdoor structural materials, vehicles, marine vessels, aircrafts, refrigerators, and many household products, to a high-quality nonfouling material. The boehmitized Al layer can also be formed on a wide range of alternative materials after applying a thin film of either vapor-deposited aluminum or sol–gel-derived alumina, thus providing a universal route for creating the same quality slippery coatings on arbitrary materials and shapes (Figure 3a). For example, starting from commercially available aluminized plastic films (e.g., PET or PP) or glass slides coated with 100 nm aluminum with a thin Ti adhesion layer, we were able to directly convert the thin aluminum layer into optically transparent SLIPS by forming boehmite before chemical functionalization and lubrication (Supporting Information Figure S3). Alternatively, we adopted a sol–gel method involving acetoacetate-stabilized aluminum tri-*sec*-butoxide solution in a mixture of isopropyl alcohol and water to prepare a thin coating of alumina on various materials.[41,42] The sol–gel method is particularly useful, as the precursor solution can be applied over a large area and on arbitrary shapes using conventional coating methods such as spray coating, spin coating, dip coating, flow coating, printing, pen writing, etc. To improve the adhesion of the sol–gel layer, the underlying substrate can be activated by plasma etching or by applying an adhesion promotion layer (see Supporting Information for details). Using this method, we have converted virtually any type of solid substrate, including glass, quartz, metals (stainless steel, copper, titanium, carbon steel), ceramics, stone, plastics (HDPE, LDPE, PP, PS, PMMA, PC, PVC, PET, polysulfone), elastomers (polyurethane, silicone), dry hydrogel, and fabrics, into robust antifouling materials. Figure 3b shows scanning electron microscopy (SEM) images of boehmite nanostructures formed on a variety of substrates. While each material shows highly uniform surface structuring, the nanoscale morphology and feature sizes of the boehmite layer produced directly on aluminum metal and those derived from the sol–gel alumina coating varies depending on the nature of the substrate, boehmitization temperature and time, and the use of steam instead of hot water. This may allow for fine-tuning of

dx.doi.org/10.1021/nl4003969 | *Nano Lett.* XXXX, XXX, XXX–XXX

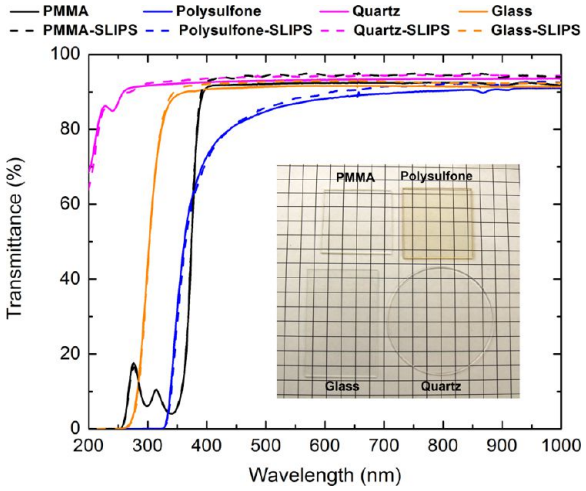

Figure 4. UV−vis spectra of unmodified substrates (solid lines) and SLIPS-coated substrates (dashed lines). The inset picture shows SLIPS-coated substrates on a square grid lines spaced 1 cm apart.

underlying nanoscale structures to further optimize the SLIPS properties.

A lubricated layer of sol−gel alumina-derived boehmite (~170 nm thick, Supporting Information Figures S4 and S5) exhibits excellent optical transparency in the range from 200 to 1000 nm, and the feature size of the nanometer scale roughness gives rise to antireflective properties (Figure 4). Supporting Information Movies 1−5 show that our robust, shear-tolerant, and optically transparent nanostructured SLIPS coatings provide many substrates with liquid-repellent, nonfouling, anti-icing, and easy-to-clean properties against a wide range of complex fluids and highly contaminating media, including hot water (>55 °C), hexadecane, ethanol, motor oil, motor oil with metallic shavings, liquid asphalt, uncured and cured cements, many of which are not repelled by the state-of-the-art superhydrophobic surfaces based on the lotus effect. In addition, SLIPS-coated substrates manufactured using our generalized methods showed extremely low ice adhesion strength (~10 kPa) that is 2 orders of magnitude lower than that of bare stainless steel (~700 kPa)[43] and Teflon (~240 kPa), and 4-fold lower than the state-of-the-art silicone-based low-ice-adhesion material (~40 kPa).[44] Moreover, these materials exhibit anticorrosive barrier layer property (Supporting Information Figure S6) and can be even bent when coated on a flexible substrate without significant deterioration of SLIPS performance.

Importantly, sol−gel alumina-derived coatings on various materials can also be patterned into nanostructured SLIPS and unstructured regions by using photocurable sol−gel alumina precursors. The methacrylate group in 2-(methacryloyloxy)-ethyl acetoacetate can be polymerized and cross-linked with an added cross-linker by photoinitiated radical generator, while the acetoacetate group can provide strong coordination to aluminum metal by replacing the alkoxy groups of the aluminum metal precursor.

Figure 5a shows an SEM image of photopatterned SLIPS on a glass substrate that only exhibits liquid-repellent behavior on certain patterned areas. We used photopatternable SLIPS coating method to create alternating rectangular areas (38 mm × 3 mm) of SLIPS and flat surface on a glass slide as shown in Figure 5b. When a water droplet was placed on this patterned substrate tilted at 30°, the droplet slid about five times faster on

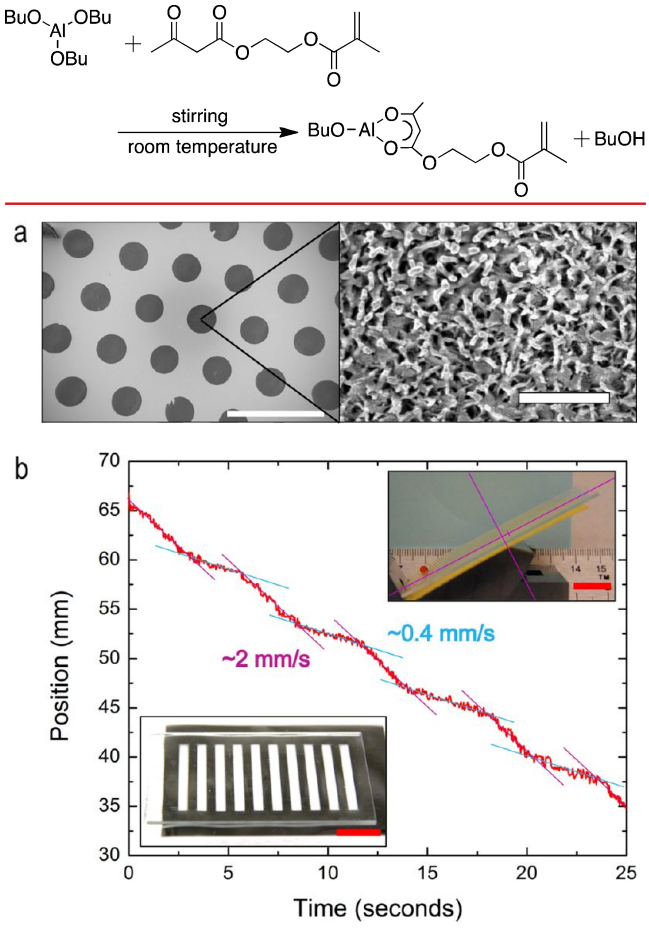

Figure 5. Patterned slippery surfaces. (a) SEM images of photopatterned sol−gel alumina-derived SLIPS on a glass slide. The dark circular areas correspond to SLIPS where the boehmite nanostructures are shown at higher magnification on the right. Scale bars are 500 μm and 500 nm, respectively. (b) Position profile of a 10 μL water droplet sliding on a substrate with alternating regions of photopatterned SLIPS and lubricated, fluorinated flat glass as shown in the bottom inset picture. The substrate is tilted at 30° as shown in the top inset picture. The droplet sliding speed repeatedly switches between ~2 mm/s (on SLIPS) and ~0.4 mm/s (on lubricated glass). Scale bars are 15 mm.

SLIPS surface than on just lubricated fluorinated flat surface (Supporting Information Movie 6). This approach will therefore allow fabrication of SLIPS-coated fluidic devices and substrates with patterns of defined wetting properties that may be useful for control of an anisotropic liquid flow and droplet motion.

In conclusion, we have shown that SLIPS coatings based solely on uniformly nanostructured surfaces provide superior performance in high-simulated shear conditions compared to hierarchically structured surfaces that are conventionally known to better perform as a Cassie−Baxter type nonwetting surface. We also have shown that robust SLIPS coatings can be formed on a variety of materials and shapes with optical transparency by creating boehmite nanostructures on the surface derived from either aluminum or sol−gel alumina overlayer. Our generalized methods of creating SLIPS offer a high level of applicability, low cost, simplicity, scalability, and compatibility with current manufacturing infrastructures and allow for converting virtually any material into an omniphobic surface

dx.doi.org/10.1021/nl4003969 | *Nano Lett.* XXXX, XXX, XXX−XXX

for many applications requiring robust antifouling, easy-to-clean, anti-ice, and anticorrosion functions.

■ ASSOCIATED CONTENT

Supporting Information

Additional information, tables, figures, and movies. This material is available free of charge via the Internet at http://pubs.acs.org.

■ AUTHOR INFORMATION

Corresponding Author

*E-mail: jaiz@seas.harvard.edu; philseok.kim@wyss.harvard.edu.

Author Contributions

P.K. and M.J.K. conceived the idea and designed the experiments. J. Aizenberg supervised the research. P.K., M.J.K, and J. Alvarenga performed the experiments and analyzed the data. P.K. and J. Aizenberg wrote the paper. All authors commented on the paper.

Notes

The authors declare no competing financial interest.

■ ACKNOWLEDGMENTS

This research was supported by the ONR under the award nos. N00014-12-1-0962 (fabrication of nonfouling surfaces on various materials) and N00014-12-1-0875 (shear-dependent behavior) and AFOSR under the award FA9550-09-1-0669-DOD35CAP (optical properties). Part of this work was performed at the Centre for Nanoscale Systems (CNS) at Harvard University, supported under NSF award no. ECS-0335765. We thank Honeywell-Sperian for providing polycarbonate lens samples and FLEXcon for providing aluminized PET sheet samples. We thank Mr. Onye Ahanotu for SEM images of sandblasted aluminum and pictures of aluminized plastic films and Dr. Alison Grinthal and Mr. Noah MacCallum for providing comments on the manuscript.

■ REFERENCES

(1) The global market for anti-fingerprint, anti-bacterial, anti-fouling, easy-to-clean and self-healing nanocoatings. In *Future Markets Technology Report*; Future Markets, Inc.: Rockville, MD, 2012.

(2) Barthlott, W.; Neinhuis, C. Purity of the sacred lotus, or escape from contamination in biological surfaces. *Planta* **1997**, *202*, 1−8.

(3) Park, K.-C.; Choi, H. J.; Chang, C.-H.; Cohen, R. E.; McKinley, G. H.; Barbastathis, G. Nanotextured Silica Surfaces with Robust Superhydrophobicity and Omnidirectional Broadband Supertransmissivity. *ACS Nano* **2012**, *6*, 3789−3799.

(4) Deng, X.; Mammen, L.; Butt, H.-J.r.; Vollmer, D. Candle Soot as a Template for a Transparent Robust Superamphiphobic Coating. *Science* **2012**, *335*, 67−70.

(5) Tuteja, A.; Choi, W.; Ma, M.; Mabry, J. M.; Mazzella, S. A.; Rutledge, G. C.; McKinley, G. H.; Cohen, R. E. Designing Superoleophobic Surfaces. *Science* **2007**, *318*, 1618−1622.

(6) Tuteja, A.; Choi, W.; Mabry, J. M.; McKinley, G. H.; Cohen, R. E. Robust omniphobic surfaces. *Proc. Natl. Acad. Sci. U.S.A.* **2008**, *105*, 18200−18205.

(7) Herminghaus, S. Roughness-induced non-wetting. *Europhys. Lett.* **2000**, *52*, 165−170.

(8) Quéré, D. Non-sticking drops. *Rep. Prog. Phys.* **2005**, *68*, 2495−2532.

(9) Chiou, N.-r.; Lu, C.; Guan, J.; Lee, L. J.; Epstein, A. J. Growth and alignment of polyaniline nanofibers with superhydrophobic, superhydrophilic and other properties. *Nat. Nanotechnol.* **2007**, *2*, 354−357.

(10) Artus, G. R. J.; Jung, S.; Zimmermann, J.; Gautschi, H.-P.; Marquardt, K.; Seeger, S. Silicone Nanofilaments and Their Application as Superhydrophobic Coatings. *Adv. Mater.* **2006**, *18*, 2758−2762.

(11) Yuan, J.; Liu, X.; Akbulut, O.; Hu, J.; Suib, S. L.; Kong, J.; Stellacci, F. Superwetting nanowire membranes for selective absorption. *Nat. Nanotechnol.* **2008**, *3*, 332−336.

(12) Ebert, D.; Bhushan, B. Transparent, Superhydrophobic, and Wear-Resistant Coatings on Glass and Polymer Substrates Using SiO_2, ZnO, and ITO Nanoparticles. *Langmuir* **2012**, *28*, 11391−11399.

(13) Sun, T.; Feng, L.; Gao, X.; Jiang, L. Bioinspired Surfaces with Special Wettability. *Acc. Chem. Res.* **2005**, *38*, 644−652.

(14) v.d. Wal, P.; Steiner, U. Super-hydrophobic surfaces made from Teflon. *Soft Matter* **2007**, *3*, 426−429.

(15) Lafuma, A.; Quéré, D. Superhydrophobic states. *Nat. Mater.* **2003**, *2*, 457−460.

(16) Liu, Y.; Chen, X.; Xin, J. H. Can superhydrophobic surfaces repel hot water? *J. Mater. Chem.* **2009**, *19*, 5602−5611.

(17) Gao, X.; Jiang, L. Water-repellent legs of water striders. *Nature* **2004**, *432*, 36.

(18) Bhushan, B.; Jung, Y. C. Natural and biomimetic artificial surfaces for superhydrophobicity, self-cleaning, low adhesion, and drag reduction. *Prog. Mater. Sci.* **2011**, *56*, 1−108.

(19) Nosonovsky, M. Multiscale Roughness and Stability of Superhydrophobic Biomimetic Interfaces. *Langmuir* **2007**, *23*, 3157−3161.

(20) Gao, L.; McCarthy, T. J. The "Lotus Effect" Explained: Two Reasons Why Two Length Scales of Topography Are Important. *Langmuir* **2006**, *22*, 2966−2967.

(21) Minko, S.; Müller, M.; Motornov, M.; Nitschke, M.; Grundke, K.; Stamm, M. Two-Level Structured Self-Adaptive Surfaces with Reversibly Tunable Properties. *J. Am. Chem. Soc.* **2003**, *125*, 3896−3900.

(22) Koch, K.; Bhushan, B.; Jung, Y. C.; Barthlott, W. Fabrication of artificial Lotus leaves and significance of hierarchical structure for superhydrophobicity and low adhesion. *Soft Matter* **2009**, *5*, 1386−1393.

(23) McCarthy, M.; Gerasopoulos, K.; Enright, R.; Culver, J. N.; Ghodssi, R.; Wang, E. N. Biotemplated hierarchical surfaces and the role of dual length scales on the repellency of impacting droplets. *Appl. Phys. Lett.* **2012**, *100*, 263701.

(24) Erbil, H. Y.; Demirel, A. L.; Avcı, Y.; Mert, O. Transformation of a Simple Plastic into a Superhydrophobic Surface. *Science* **2003**, *299*, 1377−1380.

(25) Lau, K. K. S.; Bico, J.; Teo, K. B. K.; Chhowalla, M.; Amaratunga, G. A. J.; Milne, W. I.; McKinley, G. H.; Gleason, K. K. Superhydrophobic Carbon Nanotube Forests. *Nano Lett.* **2003**, *3*, 1701−1705.

(26) Raj, R.; Enright, R.; Zhu, Y.; Adera, S.; Wang, E. N. Unified Model for Contact Angle Hysteresis on Heterogeneous and Superhydrophobic Surfaces. *Langmuir* **2012**, *28*, 15777−15788.

(27) Gao, L.; McCarthy, T. J. Contact Angle Hysteresis Explained. *Langmuir* **2006**, *22*, 6234−6237.

(28) Bocquet, L.; Lauga, E. A smooth future? *Nat. Mater.* **2011**, *10*, 334−337.

(29) Varanasi, K. K.; Deng, T.; Smith, J. D.; Hsu, M.; Bhate, N. Frost Formation and Ice Adhesion on Superhydrophobic Surfaces. *Appl. Phys. Lett.* **2010**, *97*, 234102.

(30) Wong, T.-S.; Kang, S. H.; Tang, S. K. Y.; Smythe, E. J.; Hatton, B. D.; Grinthal, A.; Aizenberg, J. Bioinspired Self-Repairing Slippery Surfaces with Pressure-Stable Omniphobicity. *Nature* **2011**, *477*, 443−447.

(31) Kim, P.; Wong, T.-S.; Alvarenga, J.; Kreder, M. J.; Adorno-Martinez, W. E.; Aizenberg, J. Liquid-Infused Nanostructured Surfaces with Extreme Anti-Ice and Anti-Frost Performance. *ACS Nano* **2012**, *6*, 6569−6577.

(32) Epstein, A. K.; Wong, T.-S.; Belisle, R. A.; Boggs, E. M.; Aizenberg, J. Liquid-infused structured surfaces with exceptional anti-

biofouling performance. *Proc. Natl. Acad. Sci. U.S.A.* **2012**, *109*, 13182−13187.
(33) Lafuma, A.; Quéré, D. Slippery Pre-Suffused Surfaces. *EPL* **2011**, *96*, 56001.
(34) Anand, S.; Paxson, A. T.; Dhiman, R.; Smith, J. D.; Varanasi, K. K. Enhanced Condensation on Lubricant-Impregnated Nanotextured Surfaces. *ACS Nano* **2012**, *6*, 10122−10129.
(35) Stone, H. A. Ice-Phobic Surfaces That Are Wet. *ACS Nano* **2012**, *6*, 6536−6540.
(36) Vedder, W.; Vermilyea, D. A. Aluminum + water reaction. *Trans. Faraday Soc.* **1969**, *65*, 561−584.
(37) He, M.; Zhou, X.; Zeng, X.; Cui, D.; Zhang, Q.; Chen, J.; Li, H.; Wang, J.; Cao, Z.; Song, Y.; Jiang, L. Hierarchically structured porous aluminum surfaces for high-efficient removal of condensed water. *Soft Matter* **2012**, *8*, 6680−6683.
(38) Furmidge, C. G. L. Studies at Phase Interfaces I. The Sliding of Liquid Drops on Solid Surfaces and a Theory for Spray Retention. *J. Colloid Sci.* **1962**, *17*, 309−324.
(39) Gutt, C.; Sprung, M.; Fendt, R.; Madsen, A.; Sinha, S. K.; Tolan, M. Partially Wetting Thin Liquid Films: Structure and Dynamics Studied with Coherent X Rays. *Phys. Rev. Lett.* **2007**, *99*, 096104.
(40) Oliver, J. F.; Huh, C.; Mason, S. G. Resistance to Spreading of Liquids by Sharp Edges. *J. Colloid Interface Sci.* **1977**, *59*, 568−581.
(41) Tadanaga, K.; Katata, N.; Minami, T. Super-Water-Repellent Al_2O_3 Coating Films with High Transparency. *J. Am. Ceram. Soc.* **1997**, *80*, 1040−1042.
(42) Ma, W.; Higaki, Y.; Otsuka, H.; Takahara, A. Perfluoropolyether-infused nano-texture: a versatile approach to omniphobic coatings with low hysteresis and high transparency. *Chem. Commun.* **2013**, *49*, 597−599.
(43) Meuler, A. J.; Smith, J. D.; Varanasi, K. K.; Mabry, J. M.; McKinley, G. H.; Cohen, R. E. Relationships Between Water Wettability and Ice Adhesion. *ACS Appl. Mater. Interfaces* **2010**, *2*, 3100−3110.
(44) Sivas, S.L.; Thomaier, R.; Hoover, K. A silicone-based ice-phobic coatings for aircrafts. 39th International Society for the Advancement of Materials and Process Engineering Technical Conference; Society for the Advancement of Materials and Process Engineering: Cincinnati, OH, 2007; pp 53−58.

dx.doi.org/10.1021/nl4003969 | *Nano Lett.* XXXX, XXX, XXX−XXX